



## Characteristics of flow through orifice-meter

Received 10 February 2024; Revised 30 March 2024; Accepted 31 March 2024

Mohamed H. Assran<sup>1</sup>  
Bakhiet Shenouda<sup>2</sup>  
Hassan I. Mohamed<sup>3</sup>

### Keywords

Coefficient of discharge,  
Orifice meter, Reynold's  
number, Triangular orifice.

### List of Notations

CFD: Computational Fluid  
Dynamics,

$k - \varepsilon$ : Turbulence model in  
Ansys Program called  
Epsilon,

$k - \omega$ : Turbulence model in  
Ansys Program called  
omega,  $L_r$ : Distance  
from the orifice to the  
ring,

$D$ : The pipe diameter

$d$ : Hydraulic diameter of the  
orifice.

*symbols not given in the above  
list are defined wherever they  
appeared.*

**Abstract:** Flow measurements in pipes and open channels are critical for successful water resource management as the economic value of water has increased. Orifice meters are typically used as flow-measuring devices in pipes because they are cheap and simple compared to other devices. Also, orifices are used as energy dissipation methods in water hammer protection devices and hydroelectric power tunnels. Although traditional circular orifice meters have been extensively studied, many points need to be studied. So, experimental and numerical research is carried out to study the effect of orifice geometry on energy loss and the discharge coefficient. The experimental tests are carried out using two different types of orifice plates: circular and triangular, for each one the cross-sectional area is changed four times. The orifice is installed on a 10 cm diameter transparent pipe. The flow rate is changed ten times for each orifice ranging from 13.8 to 49.2 m<sup>3</sup>/hr. A general correlation equation for the coefficient of discharge is deduced. It was found that the triangular orifice shapes are better than the circular orifice shapes in terms of performance, with reduced head loss and a larger discharge coefficient. By using computational fluid dynamics techniques, the flow behavior through the orifice is analyzed by ANSYS Fluent software. The numerical results confirmed the experimental ones where the pressure head loss for the triangular orifice is lower than the circular orifice and vena contracta is located at a distance equal to half the pipe diameter downstream of the orifice plate.

## 1. Introduction

Flowmeters are required in many industrial facilities and pipelines to monitor the flow rate and velocity of fluids (gas or liquid), allowing us to calculate fluid volume and its cost. Many devices, such as the orifice meter, the venturi tube, and the elbow meter, can be used to

<sup>1</sup> Teaching assistant, Building Construction dept., Arab Academy for Science and Technology (AAST), Aswan, Egypt  
[mohamed.assran88@adj.aast.edu](mailto:mohamed.assran88@adj.aast.edu)

<sup>2</sup> Lecturer, Building Construction dept., Arab Academy for Science and Technology (AAST), Aswan, Egypt.  
[eng\\_noda@aast.edu](mailto:eng_noda@aast.edu)

<sup>3</sup> Professor, Civil Engineering Dept., Faculty of Engineering, Assiut university, Assiut, Egypt. [hassan1@aun.edu.eg](mailto:hassan1@aun.edu.eg)

estimate the flow rate through pipelines, because of their simplicity and low cost. They are the most widely used flow measurement devices. However, orifice meters are the most widely used flow measurement devices for monitoring pipeline discharge. Its idea is based on measuring the pressure difference created through a pipe constriction, which changes velocity and pressure. The theoretical discharge can be determined by applying Bernoulli's Energy Equation in conjunction with the Continuity Equation. To get on the actual discharge, the theoretical discharge is multiplied by a correction factor which is called the discharge coefficient to consider the losses that occurred through the orifice meter. Many factors influence the discharge coefficient, including orifice diameter, shape, orifice hole edges, orifice plate thickness, pressure tap position, and fluid type (compressible or incompressible). Many researchers studied orifice meters from different points of view [1:4]. Prasanna et al. [5] studied the fluid compressibility impact on several orifice plate types, including the standard concentric orifice plate, quarter circle orifice plate, and square edge orifice plate. Tukiman et al. [6] and Danesh and Hassan [7] described the flow characteristics of an orifice flow meter using commercial CFD, where the flow behavior is studied and the vena contracta location is set. Krishnan et al. [8] used eight different orifice shapes to investigate the effect of orifice shapes on the coefficient of discharge. A general correlation equation for computing the discharge is deduced in this study. The orifice coefficients and discharges through circular and rectangular orifices were determined experimentally by Nicholas et al. [9], with the same cross-sectional area under a constant head of water, the rectangular orifice had a greater orifice coefficient of discharge than the circular orifice. Oliveira et al. [10] compared numerical simulation results to experimental data using Fluent software, when compared to traditional experimental procedures, the numerical methodology used was able to estimate the discharge coefficients well.

Furthermore, Imada et al. [11] compared their numerical simulation results achieved by applying the realizable  $k - \varepsilon$  and  $k - \omega$  turbulence models to the ISO Standard. It was found that the predicted discharge coefficient values agree well with the ISO Standard, with a maximum error of 4.92%, the agreement is slightly higher for the  $k - \omega$  model. Shaaban [12] added a ring downstream of the orifice, which reduced typical energy loss by 33.5 percent. Optimization studies showed that the best improvement in orifice meter pressure loss and energy consumption is obtained at a ring diameter ratio  $\beta_r = 0.5$  and a normal distance  $L_r/D = 0.38$ . Vemulapalli and Venkata [13] showed that the observed differential pressure and discharge coefficient are affected by the orifice plate thickness, pipe diameter, fluid density, edge shape, inclination angle, number of holes, position of the orifice hole, and upstream-downstream pipe lengths.

Sahin et al. [14] used a numerical model to investigate the laminar and turbulent flow characteristics of an orifice plate. In this study, the ratio of orifice plate thickness to the orifice diameter ( $t^* = t/d$ ) is varied from 1/12 to 1, while the beta ratio remains constant at 0.6,  $t^*=1$  resulted observed decrease in the pressure difference, a reduction in Cd readings, and greater

flow rate values comparing with  $t^*=1/12$ . Rahman et al. [15] investigated five orifice plates with beta ratios of 0.30, 0.35, 0.47, 0.59, and 0.71, with the hole centered in an 8.5 cm pipe diameter that is filled with water. They concluded that the orifice meter with a beta ratio of 0.60 can be used to efficiently measure pipe flow. Abd et al. [16] conducted experiments for various beta ratios and Reynolds numbers, the results showed that the Cd coefficient increases with an increase in  $\beta$  when  $Re \leq 9000$ , whereas this coefficient decreases with an increase in  $\beta$  when  $Re > 9000$ . Ahmed and Ghanem [17] used a numerical technique to consider the impacts of modifying the placement of taps, the orifice thickness ratio, and the orifice/pipe diameter ratio throughout the ranges of 0.2 to 0.8.

Almutairi et al. [18] studied the flow through a multi-hole orifice meter with three different  $\beta$  ratios 0.55, 0.6, and 0.7, Reynold's number equaled 105, it was observed that an increase in the  $\beta$  ratio causes a decrease in pressure drop and an increase in discharge coefficient. From the previous studies, it is obvious that most of them studied the circular orifice shape extensively and there are no studies concerning triangular orifice shape. Also, these studies handled the orifice as a discharge measuring device only. So, in the present study, an additional orifice of a triangular shape will be introduced and will be compared with a circular orifice from the viewpoint of discharge capacity and head loss through it.

## 2. Methods and tools

An experimental program is carried out in a hydraulic laboratory on two different shapes of orifices, i.e. circular and triangular as shown in Fig. 1. Four different sizes of each orifice shape are used of diameters or side lengths as listed in Table 1. The orifice plate with a thickness equal to 10 mm and an inclination angle equal to 45 degrees is installed through a transparent pipe of 100 mm diameter as shown in Fig. 1. The discharge through the orifice is changed ten times in the range from 13.8 to 49.2 cubic meters per hour. A mercury U-tube manometer measures the pressure difference between two taps upstream and downstream of the orifice plate at distances. The upstream tap is one time the diameter of the pipe (1D) from the orifice plate position and the downstream tap is a distance of D/2 from the orifice plate position as shown in Fig. 1 and Fig. 2.

Table 1: Range of the experimental variables

Orifices shapes	Circular				Triangular			
	Area (cm <sup>2</sup> )	32.17	23.76	15.9	8.04	31.45	23.81	16.05
Diameter or side length (cm)	6.4	5.5	4.5	3.2	8.5	7.5	6	4.5
Discharge (m <sup>3</sup> /hr)	From 13.8 to 43.4				From 14.8 to 49.2			
Pipe Reynold's number	From 51000 to 152300				From 51800 to 172750			

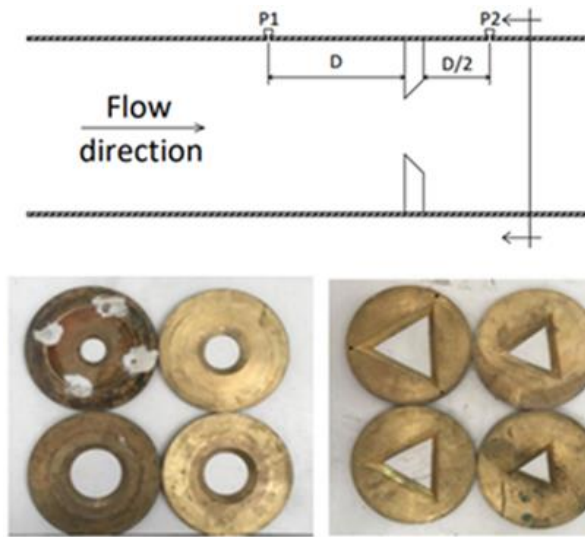


Fig. 1: Orifice plate shapes.

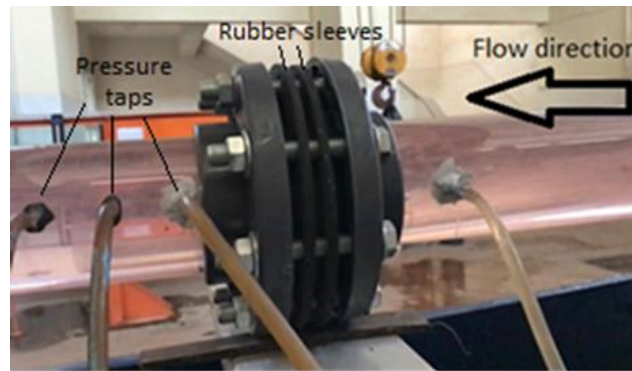


Fig. 2: Orifice meter installation through pipe.

The increased velocity of the fluid passing through the orifice produces a reduction in pressure as it passes through the hole. As the fluid exits the vena contracta, its velocity decreases and its pressure rise until it returns to its previous level. The theoretical discharge may be calculated using Bernoulli's equation by measuring the pressure head loss between the section upstream of the orifice and the section at the vena contracta. The following equation can be used for calculating the theoretical discharge through the orifice meter,

$$Q_{theoretical} = \frac{A_1 A_2 \sqrt{2gH}}{\sqrt{A_1^2 - A_2^2}} \quad (1)$$

Where  $A_1$  and  $A_2$  are the cross-sectional areas of the pipe and jet at the vena contracta, respectively, and  $H$  is the differential pressure head through the orifice. The diameter of the orifice was used to determine  $A_2$  because it was difficult to measure the diameter of the jet inside the pipe and the resulting actual value of discharge will be corrected by the discharge coefficient.

### 3. Experimental setup

#### 3.1. Dimensional Analysis

Dimensional analysis is a methodology for decreasing the quantity and complexity of experimental factors that impact a certain physical phenomenon. The goal of using dimensional analysis is to convert the various parameters to a dimensionless format to avoid dealing with a specific unit system. Saving time and money is one of the many advantages of dimensional analysis. The different variables that affect the experiment are:

- 1- Fluid characteristics (water density, dynamic viscosity, fluid velocity, .....).
- 2- Flow characteristics: (coefficient of discharge, the pressure drops, the manometer heads, pipe diameter, and discharge, .....).
- 3- Boundary characteristics: (orifice hydraulic diameter, its location plate thickness, .....), which are represented in Equation 2:
- 4-

$$C_d, \Delta P, \Delta H = f_1(D, d, \rho, \mu, v, Q) \quad (2)$$

According to the  $\pi$ -theorem principle of dimensional analysis, the parameters,  $D$ ,  $\mu$ , and  $\rho$  are defined as repeated variables and there are six variables. Then the function can be rewritten as dimensionless groups as follows in Equation 3:

$$C_d, \Delta P^*, \Delta H^* = f_2(d^*, R_e, Q^*) \quad (3)$$

Where  $\Delta P^*$  is  $\Delta P/\rho v^2$ ,  $\Delta H^*$  is  $\Delta H/d$ ,  $d^*$  is  $d/D$ , and  $Q^*$  is  $Q_{\text{theoretical}}/vD^2$ .

#### 3.2. Experiment steps.

The differential pressure head was measured by tapping a differential U-tube mercury manometer 10 cm upstream and 5 cm downstream of the orifice plate. Water was pumped into the system by a recirculating pump, and the flow rate into the pipe was controlled using a control valve. The flow discharge is measured volumetrically by the collected volume of water in a tank for a definite period. For each beta ratio, ten discharges and pressure differential readings were measured. Eight different orifice plates were set up, and for each, the actual discharges were carefully recorded. Fig. 3 shows a schematic diagram for the steps of the experiment.

#### 3.3. CFD Simulation

Computational fluid dynamics (CFD) simulation is used for flow through orifices with different shapes. CFD simulation is carried out using ANSYS Fluent software. To simulate the steady-state flow through an orifice meter, the governing equations need to be solved. In the present work, the standard k- $\epsilon$  turbulence model is used. Constant flow discharge equal to

40 m<sup>3</sup>/hr is assumed in a pipe that has a 100 mm diameter, two orifices (circular, and triangular) shapes are simulated in the pipe, and a constant area for the four shapes is taken equal to 28 cm<sup>2</sup>. The discharges and the areas are constant to comparing circular and triangular orifices under the same conditions. The mesh is generated using ANSYS Workbench with a hexahedral block organized mesh for the whole computational region (5 D upstream and 10 D downstream) as shown in Fig. 4, the number of elements is 1.2x10<sup>6</sup>.

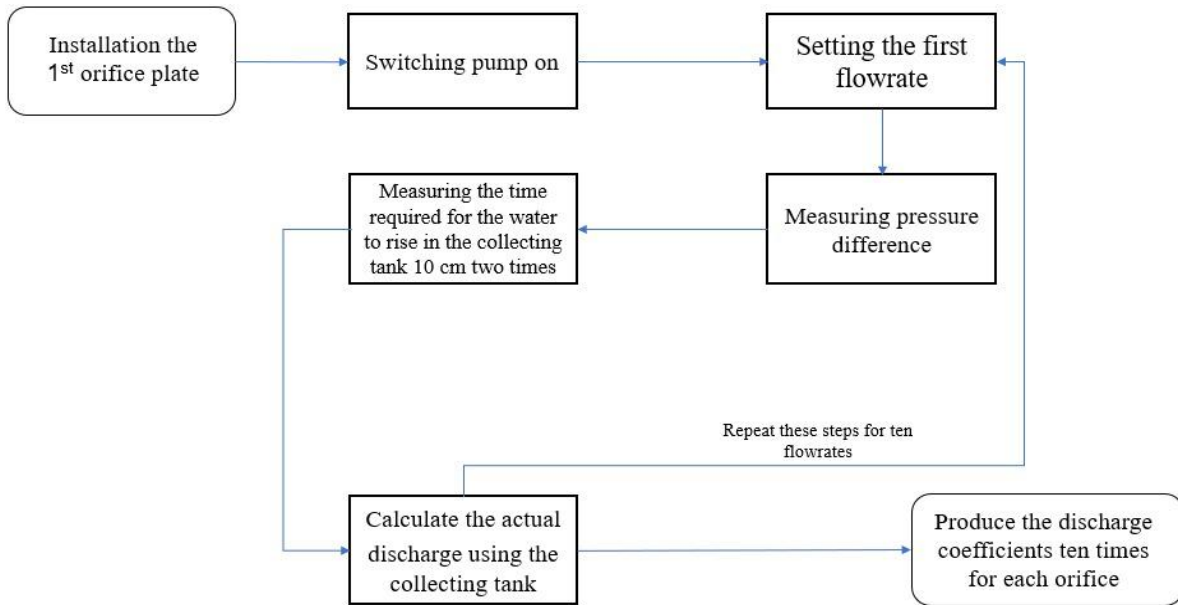


Fig. 3: Schematic diagram shows the steps of the experiment.

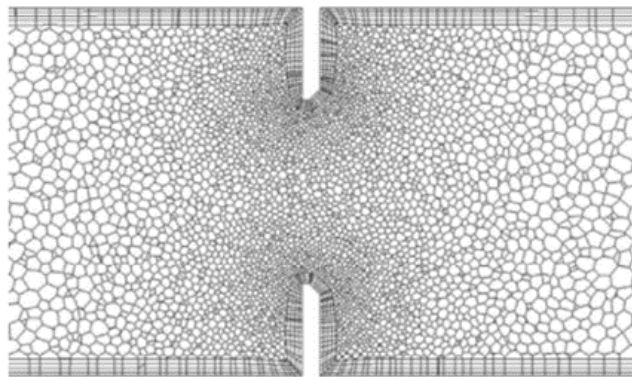


Fig. 4: Hexahedral Mesh for the study region.

#### 4. Results and Discussions

The results of the experimental program and numerical study are presented in this section. The influence of Reynold's number, orifice shape, and orifice diameter to pipe diameter ratio

on discharge coefficient and head loss through the orifice were analyzed. Based on the dimensional analysis, the studied parameters are normalized and presented in dimensionless relations.

#### 4.1. Discharge Coefficient in The Experimental Study

As shown from the previous section, many parameters affect the discharge coefficient among them Reynold's number, pressure head difference between the upstream original pipe cross-section and orifice cross-section, orifice meter shape, and the ratio of orifice meter diameter to the pipe diameter. The following effect of the different parameters on the discharge coefficient will be presented and discussed. Fig. 5 and Fig. 6 show the variation of discharge coefficient with Reynold's number at different orifice opening to pipe diameter ratios for circular and triangular shapes of orifice, respectively. For the two shapes, i.e. circular and triangular, it can be noticed that the flow was turbulent flow having Reynold's number higher than 50000. Fig. 5 shows the variation of discharge coefficient with Reynold's number for a circular orifice meter with four different orifice diameters, so the orifice diameter to pipe diameter called beta ratio ( $d/D$ ) was in the range from 0.32 to 0.64. It can be shown from the figure that there is no clear trend between the discharge coefficient and Reynold's number.

As shown in Fig. (5), for a beta ratio equal to 0.32, the relation is directly proportional, however, for a beta ratio equal to 0.45, the relation is inversely proportional, and for a beta ratio equal to 0.55 and 0.64, nearly there is no variation in discharge coefficient by increasing Reynold's number with a value of discharge coefficient equal to 0.6 for beta ratio equal to 0.55 and discharge coefficient equal to 0.58 for  $d/D$  ratio equal to 0.64. Also, it can be shown from Fig. (5) that the discharge coefficient for a circular orifice is in the range of 0.58 to 0.62, and these values are in good agreement with ISO standard values (ISO, 2003), Imada et al. [11]. Fig. 6 shows the variation of discharge coefficient with Reynold's number for triangular orifice meter with four different sizes represented as dimensionless values  $d/D$  of 0.26, 0.35, 0.43, and 0.49 respectively. For non-circular orifice meter openings,  $d$  values are taken equal to four times the hydraulic radius of the cross-section. In contrast to Fig. 5, the discharge coefficient for triangular orifice cross-section increases by increasing Reynold's number, however, there is no clear trend with beta ratio values. Also, it can be noticed that discharge coefficient values in the range of 0.62 to 0.8 which considered a high value compared to circular orifice.

As shown in the previous sections and literature review, many parameters affect the discharge coefficient, so in this section, empirical equations will be deduced for computing the discharge coefficient using approximate relations and dimensional analysis concepts. Table 2 shows the mean coefficient of discharge coefficient of various orifice shapes at different ( $A_1/A_2$ ) ratios where  $A_1$  is the cross-sectional area of the pipe and  $A_2$  is the cross-sectional area of the orifice.

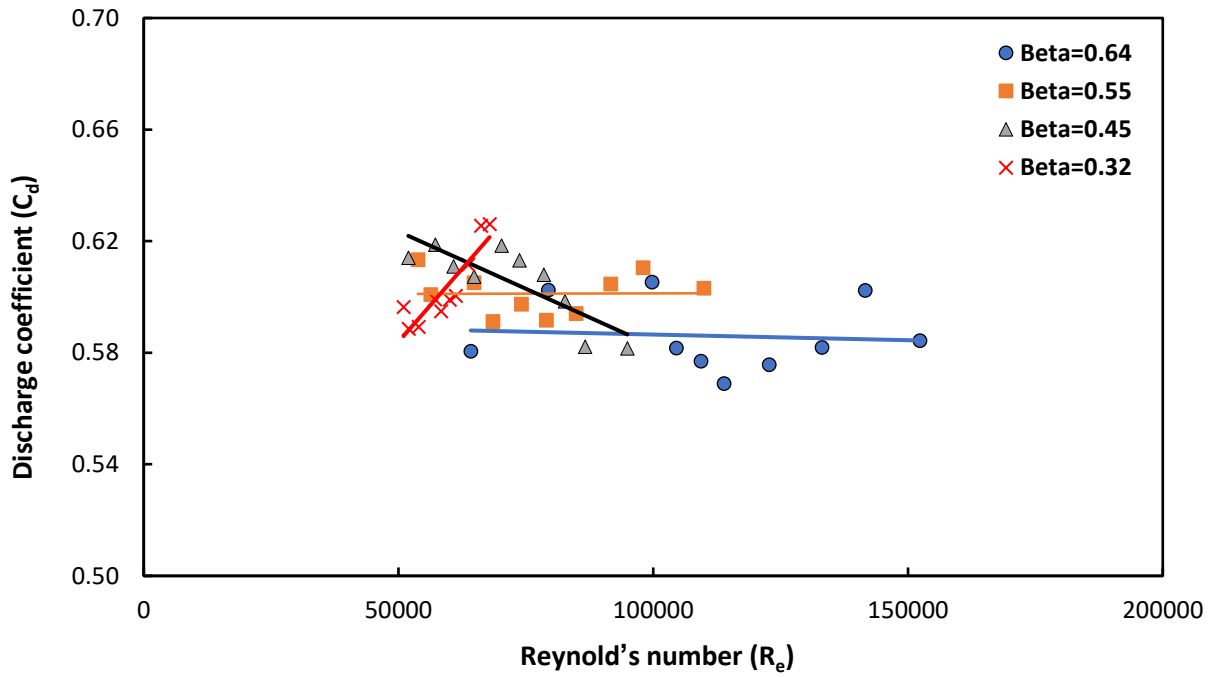


Fig. 5: Variation of  $C_d$  with Reynold's number for the circular orifices at different values of beta ratios.

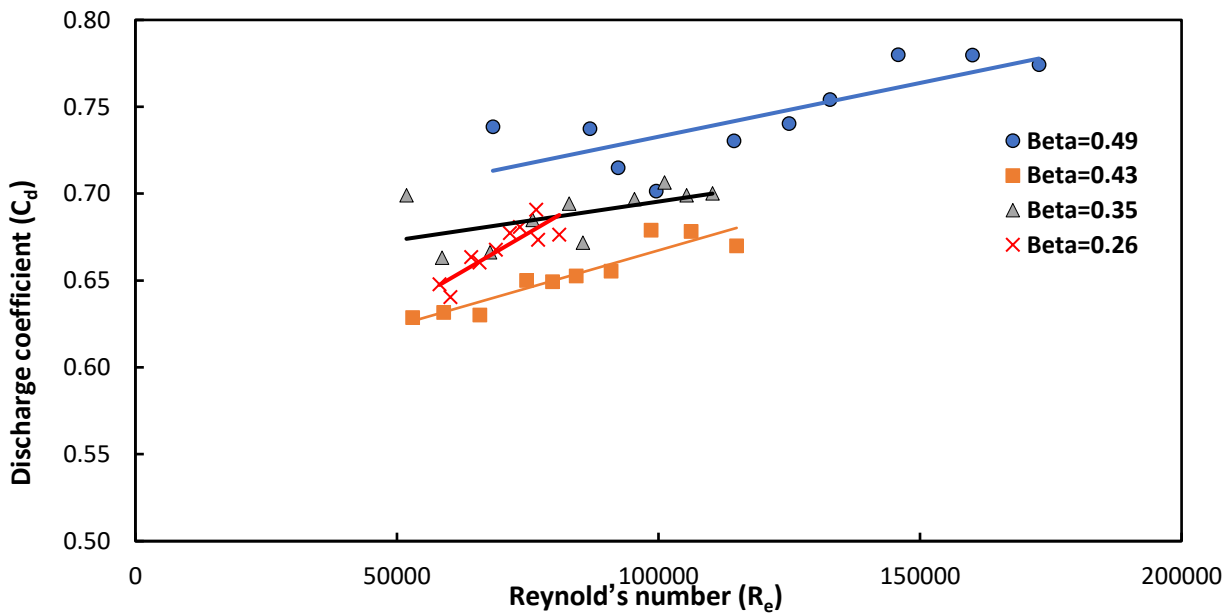


Fig. 6: Variation of  $C_d$  with Reynold's number for the triangular orifices at different values of beta ratios.

From the data in Table 2, an equation is developed for computing the discharge coefficient as a function of the ratio of the pipe cross-section area to the orifice cross-section area ( $A_1/A_2$ ) in the form of equation (4), where a, b and c are coefficients depend on the orifice shape, and its values are shown in Table 3, these coefficients are extracted from the relation between shape factor and discharge coefficient for the two orifice shapes. The maximum error from



the suggested equation does not increase by 1.1% as shown in Table 2 and the coefficient of determination  $R^2$  equals 0.994.

$$C_d = a \left(\frac{A_1}{A_2}\right)^2 - b \left(\frac{A_1}{A_2}\right) + c \tag{4}$$

Where  $A_1$  is pipe cross-sectional area,  $A_2$  is orifice cross-sectional area,  $C_d$  is coefficient of discharge and a, b, and c are constant coefficients depending on orifice shapes.

Table 2: Shape factor and average  $C_d$  of the orifices

no	Orifice shapes	Area of orifice $A_2$ (cm <sup>2</sup> )	Shape factor ( $A_1/A_2$ )	Avg. $C_d$ from Experiment	$C_d$ from correlation Equation (4)	Error %
1	C1	32.17	2.438	0.614	0.611	0.5%
2	C2	23.76	3.298	0.601	0.608	-1.1%
3	C3	15.9	4.937	0.605	0.604	0.3%
4	C4	8.04	9.813	0.603	0.607	-0.7%
5	T1	31.45	2.492	0.745	0.741	0.5%
6	T2	23.81	3.298	0.712	0.718	-0.8%
7	T3	16.05	4.876	0.688	0.685	0.5%
8	T4	8.78	8.920	0.668	0.667	0.1%

Table 3: Values of coefficient in Equation (4)

Shapes	a	b	c
Circular	0.0005	0.0066	0.6239
Triangular	0.003	0.0458	0.8368

As a function of the beta ratio and Reynold's Number, a second equation is produced for estimating the discharge coefficient. This equation matches the equation developed by Danish and Hassan [7] but with different constant values for each experimental data set. The coefficient of determination  $R^2$  for the values computed by equation (5) is 0.887.

$$C_d = 0.4768 + 0.4611\beta^{2.1} - 0.184\beta^6 \frac{0.039\beta^4}{1-\beta^4} - 0.0158\beta^3 + \frac{91.71\beta^{2.5}}{Re^{0.75}} \tag{5}$$

#### 4.2. Head Loss Through the Orifice in The Experimental Study

The head loss through the orifice is a critical parameter with various engineering applications as an energy dissipation tool, so there is a need to increase it, in some applications, there is a willingness to reduce it. Fig. 7 and Fig. 8 show the variation of head loss through the orifice as dimensionless value ( $\Delta H/d$ ) with Reynolds number at different values of the beta ratios for

circular and triangular, respectively. It can be shown that in general the head loss through the orifice increases by increasing Reynold's number and the rate of increase is higher for smaller values of the beta ratio and decreases by increasing beta ratio values.

In comparison between the figures, it can be noticed that the head loss for circular orifice is higher than that for triangular orifice. Also, it can be observed from the figures that the smaller value of the beta ratio has a different trend than the other three values for both shapes circular and triangular, when the beta ratio is less than 0.35, the head loss takes a different trend with a big increasing in the head loss. From the experimental results, an equation for determining the dimensionless head loss ( $H^* = H/d$ ) through the orifice may be obtained in the form of equation 6, where a and b are coefficients that depend on the orifice shape and beta ratio. The values of coefficients d and c are reported in Table 4.

$$\frac{\Delta H}{d} = d R_e - c \tag{6}$$

Where  $\Delta H$  is head loss, d is the hydraulic diameter of the orifices and  $R_e$  is Reynold's number.

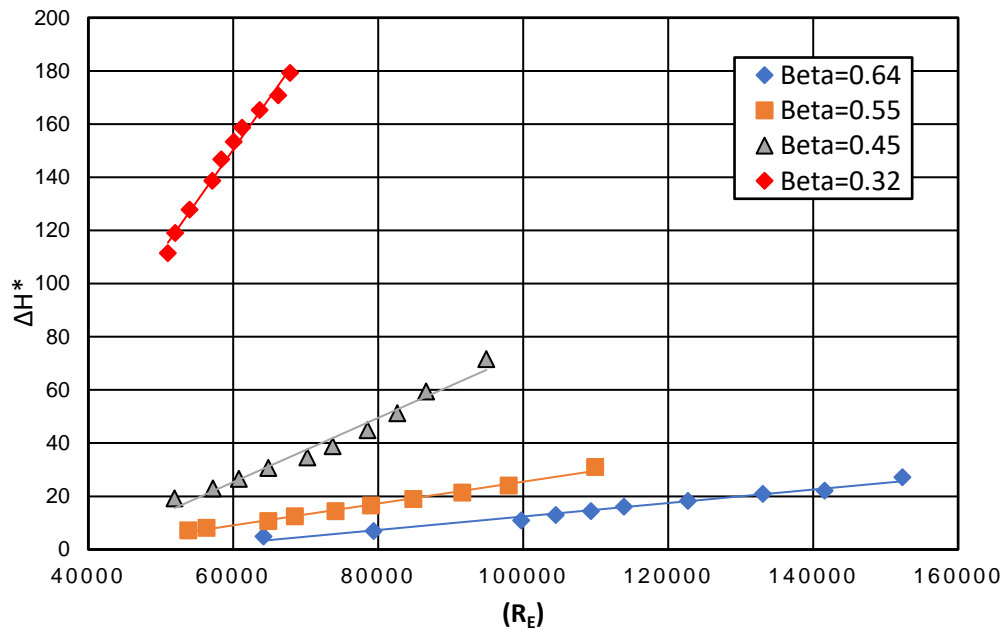


Fig. 7: Variation of head loss through the circular orifice with Reynold's number at different values of beta ratios.

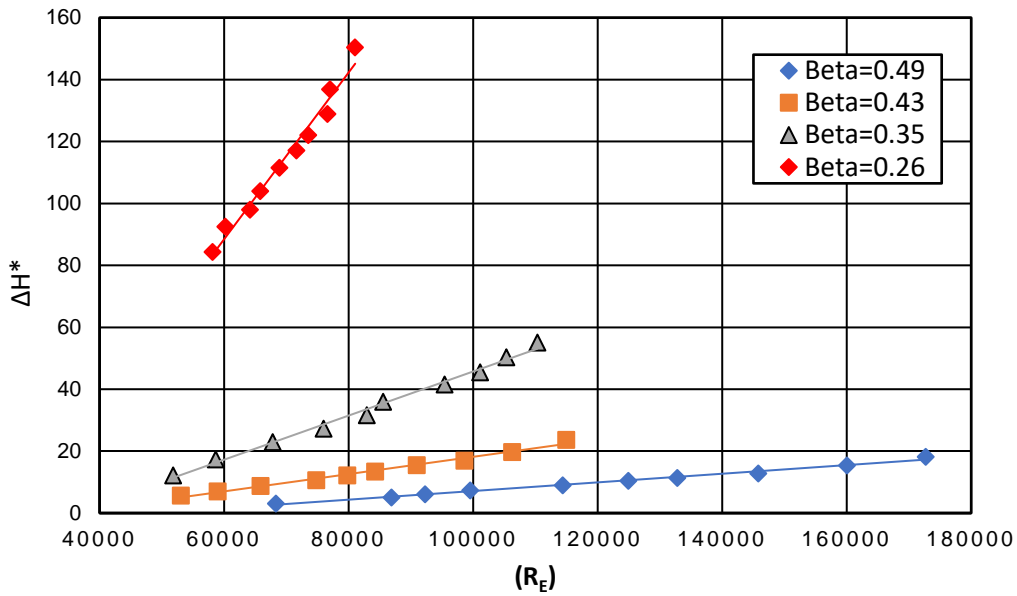


Fig. 8: Variation of head loss through the triangular orifice with Reynold’s number at different values of beta ratios.

Table 4: Values of coefficient in Equation (5)

Triangle	d/D	0.49	0.43	0.35	0.26
	d	0.0001	0.0003	0.0007	0.0027
c	6.8285	9.7397	25.478	73.044	
Circle	d/D	0.64	0.55	0.45	0.32
	d	0.0003	0.0004	0.0012	0.0039
	c	12.921	15.542	47.163	82.582

### 4.3. Numerical Results

Fig. 9 and Fig. 10 show the velocity contours of circular and triangular orifices, respectively. As shown from these figures, the high-velocity area for the triangular orifice is larger compared with the circular shapes. Also, it can be noticed from Fig. 11 that the longitudinal centerline velocity is higher for triangular orifices, which confirms the experimental results that the discharge coefficient is higher for triangular orifices. Fig. 12 shows the pressure variation along the pipe centerline for the two orifices shape. It is noticeable that the circular orifice has the higher-pressure difference, and this agrees with the experimental results. Also, it can be shown from Figs. 11 and Fig. 12, the vena contracta at about 5 cm downstream of the orifice plate which is similar to the experimental work suggestion.

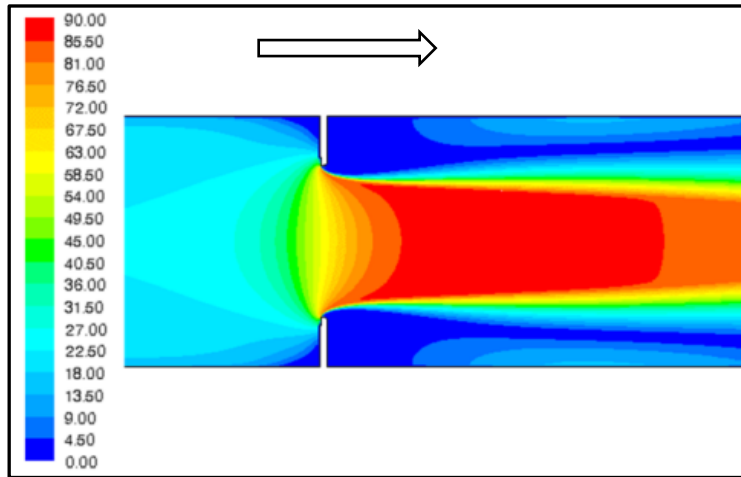


Fig. 9: Velocity contours (cm/s) for the circular orifice.

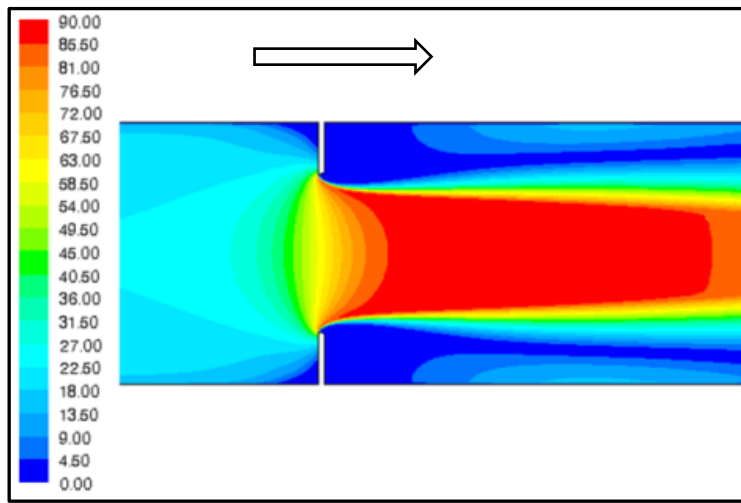


Fig. 10: Velocity contours (cm/s) for the triangular orifice.

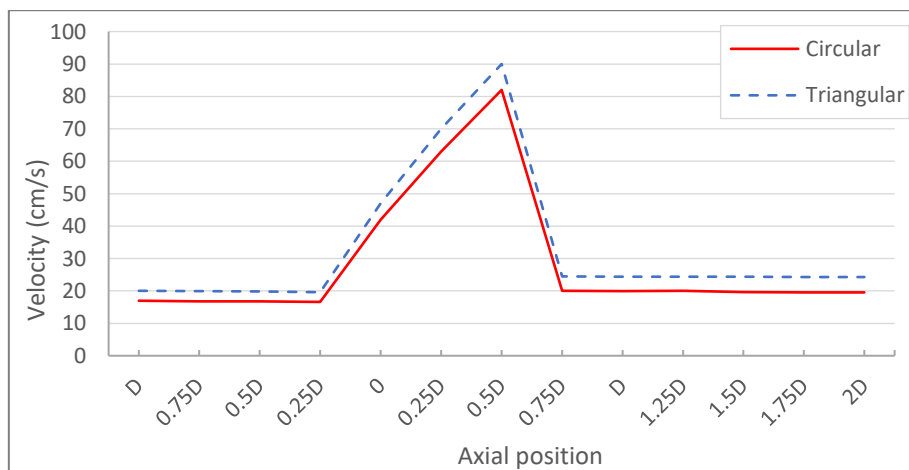


Fig. 11: The velocity variation for the two orifice shapes.

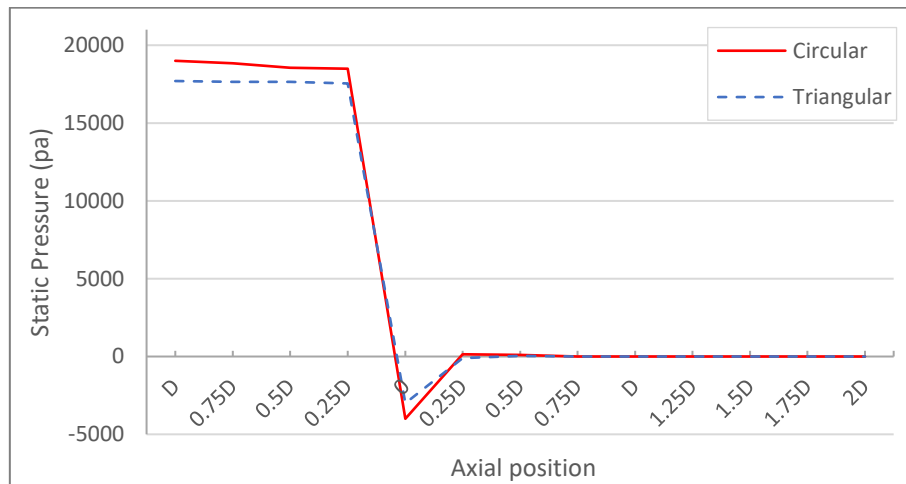


Fig. 12: The pressure variation for the two orifice shapes.

## 5. Conclusions

Write Experimental and numerical studies have been carried out for two shapes of orifice meters (circular and triangular) to investigate the effect of orifice shape on discharge coefficient and head loss through the orifice. The findings of this study can be summarized as follows.

1. For turbulent flow type of Reynold's number higher than 5000, Reynolds number has a slight effect on discharge coefficient and this effect varies with the orifice shape and the orifice diameter to the pipe ratio.
2. The value of the average discharge coefficient for triangular orifices is in the range of 0.62 to 0.8 and for circular orifices are in the range from 0.58 to 0.62.
3. The discharge for the triangular and circular orifice shapes varies linearly with the Reynolds number and independent of the orifice diameter to pipe diameter ratio.
4. The discharge increases by increasing of pressure head difference through the orifice, however, for the orifice meter with  $d/D$  less than 0.3, the rate of increase of discharge by increasing the head is small compared with the orifice meter with  $d/D$  more than 0.3 for all orifice shapes.
5. Empirical equations are deduced for computing the head loss and the discharge coefficient based on dimensional theory analysis and approximate relation for the two orifice shapes as a function of beta ratio and Reynold's Number.
6. Orifice meter with  $d/D$  less than 0.3 is more effective in energy dissipation so it is recommended to be used in surge damping.
7. Numerical analysis confirmed the experimental results where the triangular orifice has the pressure head difference and the vena contracta far from the orifice distance equal to half the pipe diameter.

## Acknowledgment

I would like to express my appreciation to all staff of the hydraulic laboratory, Faculty of Engineering, Assiut University for their cooperation during the experiments and final phase of this research.

## References

- [1] E., M. A.; and Alsaydalani, M. O., (2022) "Investigation of the discharge coefficient for orifice and pipe behavior", *Jour. Of Eng. Science and Technology*, 17 (2), pp. 839-853.
- [2] J., W.; Wanzheng, A.; and Qi, Z., (2010) "Head loss coefficient of orifice plate energy dissipator", *Jour. Of Hydr. Research*, 48 (4), pp. 526-530.
- [3] W., A.; and Tianmeng, D., (2019) "Sharp-edged orifice plate's wall pressure characteristics", *Indian Jour. Of Geo Marine Science*, 48 (6), pp. 952-956.
- [4] W., A.; and Pengfei, Z., (2021) "Correction and laboratory investigation for energy loss coefficient of square-edge orifice plate", *Science Progress*, 104 (2), pp. 1-11.
- [5] M. A. Prasanna, V. Seshadri, and Yogesh K., (2016) "Analysis of Compressible Effect in the Flow Metering by Orifice Plate Using CFD", *International Journal of Scientific Research in Science, Engineering and Technology IJSRSET*, 2 (4), pp. 170–180.
- [6] M. M. Tukiman, Ghazahi, M. N. M.; Nasir, N. F.; Nordin, N.; Sapit, A. and Razali, M. A., (2017) "CFD Simulation of Flow through an Orifice Plate", *IOP Conference Series: Materials Science and Engineering* 243, No. 1, <https://doi.org/10.1088/1757-899X/243/1/012036>.
- [7] D., M. and Hassan A., (2018) "Estimation of Discharge Coefficient in Orifice Meter by Computational Fluid Dynamics Simulation", *International Conference on Pure and Applied Sciences*, 154–56, <https://doi.org/10.14500/icpas2018.ren44>.
- [8] N. Krishnan, Ghosh, K. S.; Pradeep, K.; Divakaran, K.; Rahul, R.; and Sharun, K. S., (2017) "General Correlations of the Effect of Orifice Shapes on Coefficient of Discharge", *National Conference on Recent Innovations in Science and Engineering*, 3 (4), 53–55.
- [9] S. B. Nicholas, A. Musa and Bobai, (2018) "Determination of Orifice Coefficients for Flow Through Circular and Rectangular Orifices", *Journal of Science, Technology & Education (JOSTE)*, 6 (1), 88–97, <http://journal.stainkudus.ac.id/index.php>.
- [10] N. M.B. Oliveira, L. G.M. Vieira, and J. J.R. Damasceno, (2010) "Numerical Methodology for Orifice Meter Calibration", *Materials Science Forum* 660–661, 531–536.
- [11] F. H. J. Imada, F. Saltara, and J. L. Balino, (2013) "Numerical Determination of Discharge Coefficients of Orifice Plates and Nozzles", 22<sup>nd</sup>. *International Congress of Mechanical Engineering (COBEM 2013)*, 1755–1760, <https://www.google.com.eg/url>.
- [12] S. Shaaban, (2014) "Optimization of Orifice Meter's Energy Consumption", *Chemical Engineering Research and Design* 92, 1005–1015.
- [13] Vemulapalli, S. and Venkata, S. K. (2022) "Parametric Analysis of Orifice Plates on Measurement of Flow: A Review", *Ain Shams Engineering Journal* 13 (3), 1-23.
- [14] S., B., Akilli, H. and Tunay, T. (2004) "Investigation of Laminar and Turbulent Flow Through an Orifice Plate Inserted in a Pipe", *Transactions of the Canadian Society for Mechanical Engineering*, 28 (2), 403–413.

- [15] M. Rahman, R Biswas, and W. I. Mahfuz, (2009) "Effects of Beta Ratio and Reynold's Number on Coefficient of Discharge of Orifice Meter", *Journal of Agriculture & Rural Development*, 7, 151–156.
- [16] H. M. Abd, O. R. Alomar, and I. A. Mohamed, (2019) "Effects of varying orifice diameter and Reynolds number on discharge coefficient and wall pressure", *Flow Meas. Instrum.*, vol. 65, pp. 219–226, doi: 10.1016/j.flowmeasinst.2019.01.004.
- [17] E. N. Ahmed and A. A. Ghanem. (2020), "A novel comprehensive correlation for discharge coefficient of square-edged concentric orifice plate at low Reynolds numbers", *Flow Measurement and Instrumentation*, 73, <https://doi.org/10.1016/j.flowmeasinst.2020.101751>.
- [18] J. Almutairi, A. Hasečić and E. Džaferović (2023) "Numerical Analysis of Newtonian Fluid Flow Through Multi-Hole Orifice Meter", the 9<sup>th</sup>. World Congress on Mechanical, Chemical, and Material Engineering (MCM'23).

## خصائص تدفق المياه من خلال فوهة المقياس

تعتبر قياسات التدفق عبر الأنابيب والقنوات المفتوحة مهمة جدًا لإدارة موارد المياه والصناعة. مقياس الفوهة هو جهاز قياس التدفق شائع الاستخدام على نطاق واسع في الأنابيب لأنه رخيص جدًا وبسيط مقارنة بالأجهزة الأخرى، ومع ذلك هناك العديد من المعاملات التي تؤثر على أدائه مثل شكل الفوهة وقطر الفوهة وسماكة الفوهة ورقم رينولد الذي يعتمد على كمية التصرف وسرعته ونوع المائع ولزوجة المائع، أيضًا يتم استخدام الفوهة كطريقة لتبديد الطاقة في أجهزة حماية ظاهرة المطرقة المائية التي تحدث في أنفاق الطاقة الكهرومائية. على الرغم من سهولة تركيبها في خط الأنابيب فإن العيب الرئيسي لمقياس الفوهة هو أنها تفقد المزيد من الطاقة بسبب الاحتكاك والانكماش والانسداد والدوامات وما إلى ذلك مقارنة بأنبوب الفنشوري القياسي أو فوهة التدفق متغيرة القطر. يعوق مقياس الفوهة تدفق المائع في الأنبوب ويسبب ذلك فرقًا في الضغط على جانبي فوهة المقياس ونتيجة لذلك يتم حساب التصرف النظري باستخدام معادلة برنولي. لذلك تم إجراء بحث عملي من خلال تجارب معملية في معمل الري والهيدروليكا بكلية الهندسة - جامعة أسيوط لدراسة تأثير عدة أشكال من مقياس الفوهة على فقد الطاقة ومعامل التصرف، بسبب فقد الطاقة التي يحدث على جانبي مقياس الفوهة يتم حساب معامل التصرف من ناتج قسمة التصرف الفعلي على التصرف النظري. تم إجراء الاختبارات المعملية باستخدام شكلين مختلفين من فوهات المقياس التصرف، هذه الأشكال هي: فوهة دائرية وفوهة مثلثة. تم تغيير مساحة المقطع لكل شكل أربع مساحات مختلفة، هذه التجارب أجريت على أنبوب شفاف قطره ١٠ سنتيمتر وتم تغيير معدل التدفق خلال الأنبوب عشر مرات لكل نوع من أشكال مقياس الفوهة بإجمالي عدد مائة وستون تجربة.

تم قياس فرق الضغط بين جانبي مقياس الفوهة باستخدام مانومتر زئبقي تم توصيله من خلال ثقب تقع على جانبي الفوهة على مسافة تساوى قطر الأنبوب في الجانب التي يأتي منه التدفق أمام فوهة المقياس والثقب الآخر يقع على مسافة تساوى نصف قطر الأنبوب في الخلف. هذا ملخص لأهم النتائج والتوصيات التي تم التوصل إليها من هذا البحث وتم تلخيصها كالآتي:

(١) بالنسبة لنوع التدفق المضطرب لرقم رينولد الأعلى من ٥٠٠٠، فإن رقم رينولد له تأثير طفيف على معامل التصرف وهذا التأثير يختلف باختلاف شكل الفوهة وقطر الفوهة إلى نسبة الأنبوب.

- (٢) أعلى قيمة لمتوسط معامل التصرف هي للفوهة المثلثة في المدى من ٠,٦٢ إلى ٠,٨.
- (٣) أصغر قيمة لمتوسط معامل التصرف هي للفوهة الدائرية في المدى من ٠,٥٨ إلى ٠,٦٢.



- ٤) يتنوع معامل التصرف لجميع أشكال الفوهة خطياً مع رقم رينولد لجميع أشكال الفوهة ومستقلاً عن نسبة قطر الفوهة إلى قطر الأنبوب.
- ٥) يزداد معامل التصرف بزيادة فرق الضغط خلال الفوهة، ومع ذلك بالنسبة للفوهات ذات الحجم الصغير، يكون معدل زيادة معامل التصرف عن طريق زيادة فرق الضغط صغيراً مقارنة بحجم الفوهة الكبيرة لجميع أشكال الفوهة.
- ٦) تم استنتاج المعادلات التجريبية لحساب معامل التصرف بناءً على تحليل نظرية الأبعاد والعلاقة التقريبية لأشكال الفوهات المختلفة كدالة في نسبة المساحة ونسبة بيتا ورقم رينولد.

$$C_d = a \left( \frac{A_1}{A_2} \right)^2 - b \left( \frac{A_1}{A_2} \right) + c$$

$$C_d = 0,4768 + 0,4611\beta^{2,1} - 0,184\beta^6 \frac{0,039\beta^4}{1 - \beta^4} - 0,0158\beta^3 + \frac{91,71\beta^{2,5}}{Re^{0,75}}$$

- ٧) يعتبر مقياس الفوهة ذات نسبة بيتا أقل من ٠,٣ أكثر فاعلية في تبديد الطاقة لذلك يوصى باستخدامه في التخمين المفاجئ.
- ٨) تم استنتاج معادلة لحساب فرق الضغط على جانبي الفوهة.

$$\frac{\Delta H}{d} = a R_e - b$$

- ٩) شكل الفوهة المثالية لديه أعلى سرعة تدفق وأعلى معامل تصرف عند استخدام الطريقة النظرية بالبرامج.
- ١٠) يزداد معامل التصرف بزيادة عدم انتظام شكل الفوهة وقد يكون ذلك بسبب تقليص المنطقة الميتة خلف الفوهة.